M. B. C. Pinto, R. A. C. Ghion and F. L. Schmidt

Machine Learning Approach to Enhancing Drying Efficiency of Hop (*Humulus lupulus* L.)

Beer is the most produced alcoholic beverage in the world with a production of 1.82 billion hectoliters in 2020, in which hops remain one of the most important raw materials. Hops drying stands as a key step to reduce the moisture right after the harvest, avoiding deterioration. Drying remains an issue due to a lack of process control, high energy demand, and consequently greenhouse gas emissions. This study intends to probe into the viability of computational modeling for time prediction to optimize the drying step of processing. For that, KNN, ANN, and Random Forest algorithms were compared with conventional empirical models according to statistical error and accuracy. From the outcomes, it was constructed a model with high accuracy $R^2 > 0.999$ using the KNN and Random Forest algorithms. It demonstrates higher accuracy in comparison with conventional mathematical models as well as a simple and more rapid time prediction. The new tool developed and tested in this study enables the reduction of drying time by a model using wider process variables. Consequently, the product quality is enhanced, and the drying footprint might be reduced by more effective energy usage.

Descriptors: kilning, machine learning, modeling prediction, artificial neural network

1 Introduction

Beer is the most produced alcoholic beverage in the world, with a production of 1.82 billion hectoliters in 2020 [1]. The main raw materials are barley malt, yeast, water, and hops [2]. Hop is an important ingredient in beer, adding flavor through its unique bitter compounds and essential oils [3]. New hopping techniques, such as dry hopping, and an increase in hoppy beer consumption have led to hop production growth in the past decades, reaching 62,366 ha of hop cultivation in 2020 [4]. Furthermore, higher demand for the addition of hops widely impacts the environment due to greenhouse gas emissions during its cultivation and processing. Hop production is responsible for emitting 3.5 to 5.5 kg of CO_2 per kilogram of hops, as a sum of the footprint of agricultural machinery, pesticides, fertilizers, and drying [5].

The moisture of fresh cones is reduced by drying on the farm right after picking [6]. However, hop drying requires massive energy consumption, impacting greatly on hop processing footprint. This step is crucial to enhance quality during storage, avoiding mold potential, which can lead to microbiological deterioration [5, 7]. Reducing the drying time might be one key to CO_2 mitigation in hop production. Furthermore, an optimized drying process leads to product quality enhancement by avoiding over-maturation of hop cones.

The food drying process involves a complex matrix with physico-chemical transformation and structural changes [8]. Therefore, the drying process optimization is rarely obtained by empirical mathematical models. Several empirical models have been developed in the past decades to predict drying process variables, such as temperature, drying rate, and moisture rate. However, those models are limited regarding time prediction [9–13]. Machine learning application offers several advantages when compared with empirical modeling techniques due to their ability to adjust non-linear functions, learning suitability, and flexibility to numerous systems [14]. Among those, Artificial Neural Networks (ANN), Random Forest, and K-Nearest Neighbor (KNN) have been widely used in food research to optimize food processing, such as fruit drying, detect fraud in food matrices, and control food product quality [15–19].

To date, no studies have been found using the machine learning approach to predict drying time, despite this method being already explored in moisture content prediction [18, 19, 21, 40]. Therefore, this study benefits from the advantages of using computational tools as an alternative to empirical mathematical models. Considering the challenge of hop farms in controlling the drying process, this study aims to propose a novel method to predict the drying time of hops by using machine learning techniques to build a more accurate model including a wider range of drying parameters. Those models were developed using drying absolute temperature, wet-bulb temperature (air temperature measured by a thermometer bulb surrounded by a wet cloth), dry-bulb temperature (air temperature measured by a thermometer bulb), and moisture. They offer an alternative tool for process optimization and control, leading to energy efficiency improvements and, consequently, reduction of greenhouse gas

https://doi.org/10.23763/BrSc23-02pinto

Authors

Mariana Barreto Carvalhal Pinto, Rafael do Amaral Campos Ghion, Flavio Luis Schmidt, Fruit and Vegetables Laboratory – Department of Food Technology, School of Food Engineering, University of Campinas (UNICAMP), Campinas, SP, Brazil; corresponding author: maribcarvalhal@gmail.com

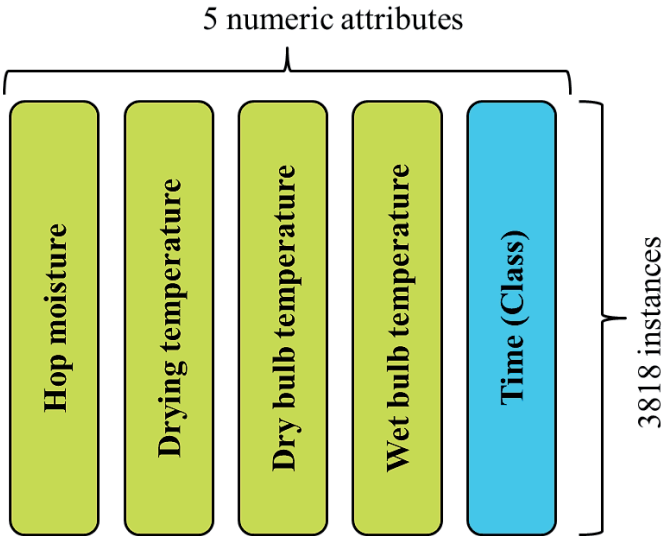

Fig. 1 Machine learning dataset composition

emissions. In addition, more precise drying time control reduces post-harvest waste on the farms due to the faster process.

2 Materials and Methods

This study compares the five classic empirical models used in the drying process with the three most common machine learning algorithms trained and tested with the same experimental dataset. The dataset was randomly split into training (70 %) and testing groups (30 %). It was composed of the 5 numeric attributes (including time as a class) and 3818 instances (Fig. 1). The empirical and machine learning models were compared according to the R^2 and Root Mean Square Error (RMSE). The detailed methodology for data collection, drying experiment, and the machine learning models' parameters are in the following sections.

2.1 Drying experiment

To collect the experimental data on the drying process for the models' construction, Brazilian hops (*Humulus lupulus* L.) variety 'Mantiqueira' was used in the present study. All cones were dried in triplicate at 70, 55, and 40 °C with an air velocity of 6.6 m/s and volumetric airflow of 0.013 m³/s. The air temperatures were measured using fixed-type T thermocouples (Ecklund-Harrison, USA) installed inside and outside of the drier. All thermocouples were connected to a data logger (Almemo 2890-9, Ahlborn, Germany), and data were analyzed using a Microsoft Excel® spreadsheet. As shown in figure 2, the trials were carried out in three perforated (mesh 14, wires 30 mm) 314 stainless steel 30 × 20 × 10 cm baskets placed in model MA035 oven drier (Marconi, Piracicaba, Brazil). Each batch was performed with three baskets containing 100 g of hops each. The hop's weight was measured during the drying process by one of the baskets linked to a weight balance connected to a PC, acquiring the data every minute by self-developed software. The moisture content was analyzed following the Hops-4 ASBC (American Society of Brewing and Chemists) [20] method adapted using 1 g of sample dried in an oven drier for 2 hours at 105 °C.

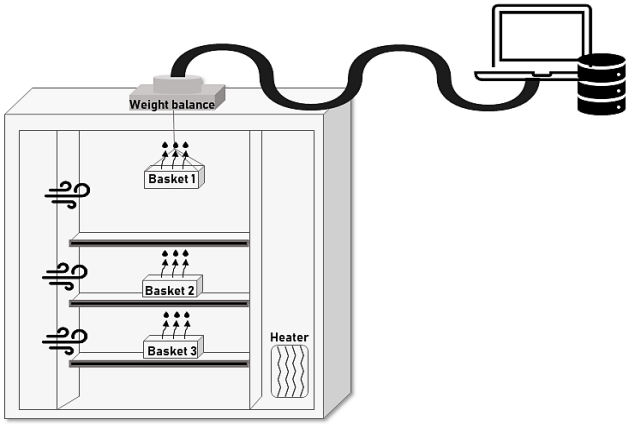

Fig. 2 Diagram of drying experiment with data collection

The moisture rate (MR) is a dimensionless value that was calculated according to equation 1.

$$MR = \frac{X - X_{eq}}{X_0 - X_{eq}} \quad \text{(Eq. 1)}$$

Where, X, X_{eq} an,d X_0 correspond to average moisture content at weighting time (g/g_{solids}), average equilibrium moisture content ($g/_{gsolids}$), and average initial moisture content (g/g_{solids}), respectively [22]. The equilibrium moisture content was determined by drying a hops batch until a constant weight was achieved, which is characterized as in equilibrium.

2.2 Effective Moisture Diffusivity and Activation Energy Determination

The effective moisture diffusivity was calculated by Fick's law, assuming diffusion as the principal mechanism of water transfer [23].

$$\frac{\partial Mt}{\partial t} = \nabla \cdot (D_{eff} \nabla M_t) \quad \text{(Eq. 2)}$$

The equation 3 solution arises with the assumption of uniform initial moisture distribution, constant diffusion, and a spherical shape during drying:

$$MR = \frac{Mt - Me}{Mb - Me} = \frac{6}{\pi^2} \sum_{n=1}^{\infty} \frac{1}{2n^2} \exp\left(-n^2 \pi^2 \frac{Deff \cdot t}{r_e^2}\right) \quad \text{(Eq. 3)}$$

where n is the polynomial coefficient, t is the drying time (s), r_e is the sample radius (m), and D_{eff} is the effective moisture diffusivity (m^2/s).

For the extended drying process, Equation 3 could be simplified to the first term, resulting in equation 4.

$$MR = \left(\frac{6}{\pi^2}\right) \exp\left(-\pi^2 \frac{Deff \cdot t}{r_e^2}\right) \quad \text{(Eq. 4)}$$

Equation 5 represents the linear relation of equation 4 after logarithmic transformation.

$$\ln(MR) = \ln\left(\frac{6}{\pi^2}\right) - \left(-\frac{Deff \cdot \pi^2 \cdot t}{r_e^2}\right) \quad \text{(Eq. 5)}$$

The diffusivity coefficient (K_1) was obtained from the ln (MR) × time plotted chart, resulting in equation 6.

$$K_1 = \left(\frac{Deff \,.\, \pi^2}{{r_e}^2}\right) \quad \text{(Eq. 6)}$$

The activation energy was calculated based on the Arrhenius equation from the relationship between effective moisture diffusivity and the average temperature.

$$\mathrm{D_{eff}} = D_0 \, \exp\left(\frac{E_a}{R_g \,.\, T_a}\right) \quad \text{(Eq. 7)}$$

where T_a is the absolute air temperature (K), R_g is the gas constant (8,3143 kJ/mol), D_0 is the pre-exponential factor, and E_a is the activation energy (kJ/mol). The linear relation of equation 7 results in equation 8.

$$\ln\left(\mathrm{D_{eff}}\right) = \left(\frac{E_a}{R_g \,.\, T_a}\right) + \ln\left(D_0\right) \quad \text{(Eq. 8)}$$

The activation energy coefficient (K2) was obtained from the slope of ln (D_{eff}) × $\frac{1}{T_a}$ plotted chart, resulting in equation 9.

$$K_2 = \frac{E_a}{R_g} \quad \text{(Eq. 9)}$$

2.3 Empirical mathematical modeling

Five of the most used mathematical models for drying were selected to compare with the model built by machine learning (Table 1). Those models contain the moisture rate as a function of time and the constants are calculated by fitting the experimental data.

2.4 Machine Learning Methods

Three models of machine learning were tested and compared to the mathematical ones: Artificial Neural Network, Random Forest, and K-Nearest Neighborhood. Here, is proposed their usage to predict the drying time of hops. These algorithms were selected due to their efficiency and malleability in prediction, being widely used for decades in health research for disease development prediction, demonstrating the suitability of the machine learning tools [24–29].

The machine learning models were built as the input attributes of the absolute temperature (°C), wet-bulb temperature (°C), dry-bulb temperature (°C), moisture content (g_{water}/g_{solids}) and drying time (s) as a class. The model was constructed with 3819 instances through cross-validation with 10 folds.

Artificial Neural Network: This model was built using the classifier Multilayer Perceptron at Weka® (version 3.9.4, Hamilton, New Zealand) which uses backpropagation to teach a multi-layer perceptron to classify instances. It is named weka.classifiers.functions.MultilayerPerceptron. The dataset was trained and tested through Cross-validation with 10 folds. Since the class is numeric, the output nodes have non-thresholded linear units. The network parameters were modified to achieve higher model fitting. The algorithm was set to normalize the attributes and the numeric class to improve network performance. The momentum applied to the weight updates was 0.2, the number of decimal places used for the output of numbers in the model was 2, the learning rate for weight updates was 0.3, and the batch size, which is the preferred number of instances to process if the batch prediction is being performed, was 100 instances. The number of seeds was optimized to achieve higher network performance. This model used 4 seeds to initialize the random number generator. The hidden layers of the neural network were set as 't' which means the number of attributes + classes.

Table 1 Empirical Mathematical Drying Model

Model Name	Equation	References
Newton	MR = exp (-kt)	[9]
Page	MR = exp (-kt^n)	[10]
Logarithmic	MR = a exp (-kt) + c	[11]
Two terms	MR = a exp (-k_1t) + b exp (-k_2t)	[12]
Henderson e Pabis modified	MR = a exp (-kt) + b exp (-gt) +c exp (-ht)	[13]

Random Forest: The model was built using the classifier Random Forest at Weka® (version 3.9.4, Hamilton, New Zealand) which is a special case of boosting meta classifier constructed by a forest of random trees [30]. It is named weka.classifiers.trees.RandomForest. The dataset was trained and tested through Cross-validation with 10 folds. The trees parameters were the default of Weka with the random number seed used as 1, the number of execution slots (threads) to use for constructing the ensemble as 1, the size of each bag as 100, and the number of decimal places to be used for the output of numbers in the model as two, the batch size set as 100, the number of trees in the random forest as 100, and the tree depth set as unlimited.

K-Nearest Neighbor: The model was built using the K-nearest neighbors classifier at Weka® (version 3.9.4, Hamilton, New Zealand) which is named weka.classifiers.lazy.IBk [31]. The dataset was trained and tested through Cross-validation with 10 folds. The K value selection was based on cross-validation, using the meta classifier Cross-validation Parameter selection (weka.classifiers.meta.CVParameterSelection) [32]. The classifier parameters were used by the software default with one random seed, 10 folds used for cross-validation, two decimal places to be used for the output of numbers in the model, batch size of 100 instances, and the scheme parameters set to cross-validation "K 1 10 10". The regression with the KNN classifier was performed using the 2 nearest neighbors, as selected by cross-validation, Euclidean distance, batch size of 100 instances, the output of numbers in the model set as two decimal places, and window size set as 0, which means there was no limit to the number of training instances.

3 Bitter acid analyses

3.1 Sample preparation

Samples of fresh and dried cones were lyophilized for 24 hours to eliminate residual water and milled using liquid nitrogen to avoid oxidation reactions. The analysis was carried out in triplicate for each sample. For bitter acid extraction, 20 mL methanol was added to 250 mg of hop powder (acidified with 0.01 % formic acid) in a falcon tube and agitated for 1 hour. The samples were centrifuged (Laborline, Barueri, Brazil) for 5 min at 700 ×g and an aliquot of 5 mL of supernatant was withdrawn and transferred to an amber

glass tube. The samples were filtered using a 0.45 µm cellulose filter supplied by Sinergia Científica (Campinas, Brazil) and followed by HPLC (High-Pressure Liquid Chromatography) analysis.

3.2 HPLC analysis

The α- and β-acid contents were determined by HPLC (Waters Corporation, Milford, USA), according to the method adapted from *Keukeleire* et al. (2003) and Hops-14 ASBC (American Society of Brewing and Chemists, 2008). The column used for compound separation was a C-18 column (SunFire, 250 × 4.6 mm, 5 µm; Water Corporation, Milford, USA). Chromatographic conditions consisted of an isocratic gradient composed of 15 % eluent A (milli-Q water acidified with 1.47 % (v/v) phosphoric acid 85 %) and 85 % of eluent B (HPLC-grade methanol). The injection volume was 10 µL using a Waters 717 plus autosampler. The flow rate was 1 mL/min, the run time was 50 min, and the column temperature was 25 °C. The detection was at 314 nm for α- and β-acids and 370 nm for xanthohumol using the Waters 996 photodiode array detector. The retention time comparison with an external standard (ICE-4 and xanthohumol 60 % Standard), also applied for quantification of α-, β-acids, and xanthohumol determined the identification of the peaks.

3.3 Surface Color Measurement

The surface color of samples was determined by a portable colorimeter MiniScan XE (Hunter Associates Laboratory, Inc., Reston, Virginia, USA), with enlightening D65 and an observation angle of 10°. The CIE Lab color parameters, i.e., L* (whiteness or brightness), a* (redness or greenness), and b* (yellowness or blueness) coordinates, were used to describe the color of samples. Color measurements were taken in triplicate.

3.4 Total Essential Oil Content

Total oil content was determined using hydro-distillation, following the methodology described by ASBC (American Society of Brewing and Chemists, 2011b). 100 g of fresh and dried hops were submitted separately to hydro-distillation for 4 h using a Clevenger apparatus.

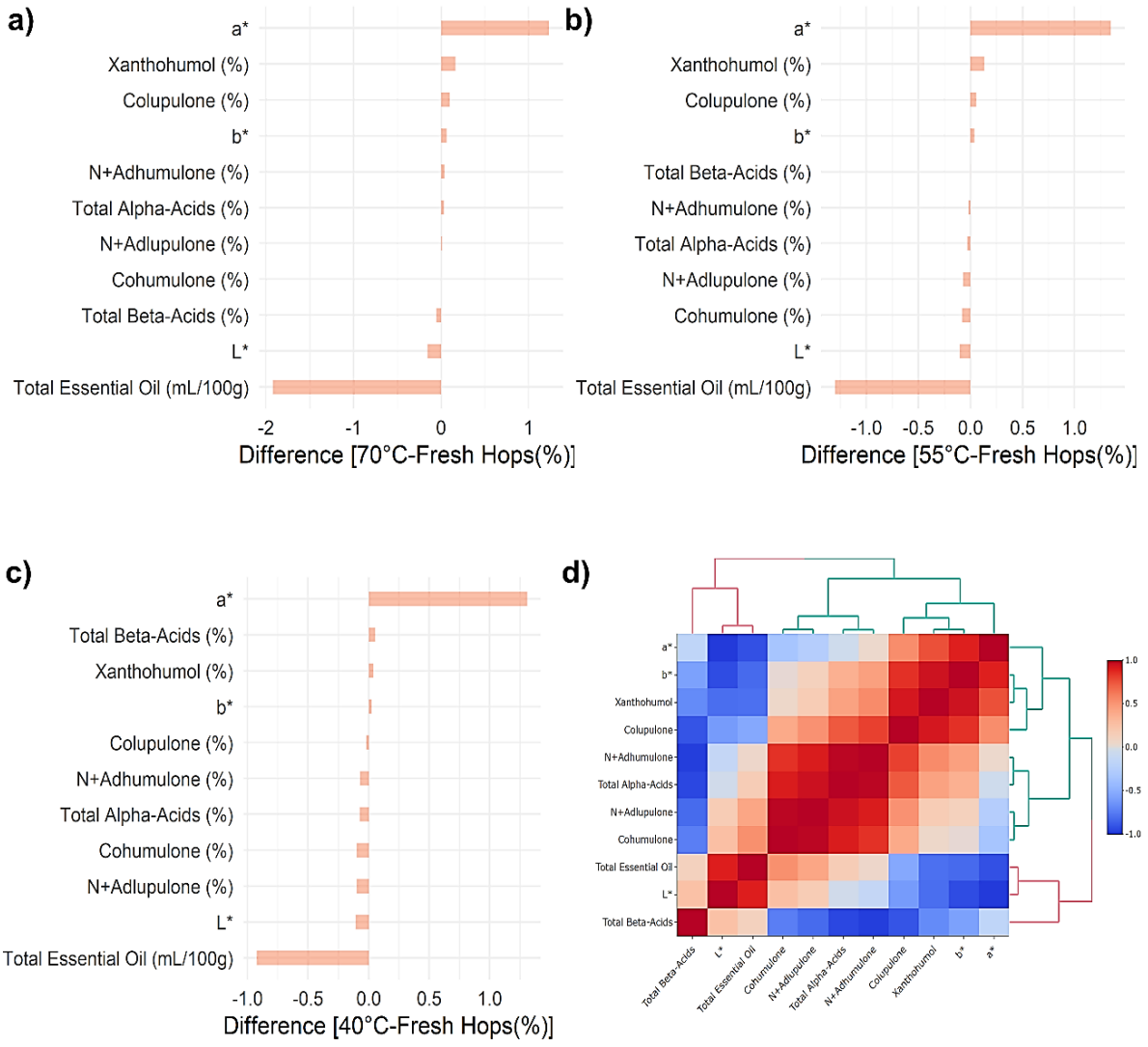

Fig. 3 Overall influence of drying temperature on the main hop quality parameters: a) Difference between fresh hop and dried at 70°C*; b) Difference between fresh hop and dried at 55°C*; c) Difference between fresh hop and dried at 40°C*; d) Correlogram constructed from Pearson's correlation (* L*, a*, and b* corresponding to color CIELAB parameters: L* value indicates lightness, a* and b* are chromaticity coordinates; **Detailed data is available in Supplementary Material (Table S2))**

The volume of oil was observed in the receiver.

3.5 Statistical analysis

The temperature (40, 55, and 70 °C) effects on hop chemical analytes were evaluated by a percentual difference calculated between fresh and dried hops and presented in a bar plot constructed using RStudio (Package: ggplot). Pearson's correlation between the results was performed in RStudio (Package: Heatmaply). The drying curves modeling by the empirical models was performed by non-linear regression analysis using Origin software (version OriginPro 2020b). The experimental data were fitted with the empirical mathematical models, obtaining R^2 and root mean square error (RMSE) values which were used to evaluate the model's fit to the dataset.

4 Results and Discussion

4.1 Effect of drying process on hop quality

The drying process substantially affects food matrices due to higher temperature or processing time applications. Figure 3 shows the overall modification of hop quality during drying at each temperature. The results of the main hop quality parameters were evaluated as a percentual difference in the values between the applied temperature and fresh hops (Fig. a-c) and Pearson's correlation through a correlogram (Fig. d). A percentual difference between the trials was chosen to facilitate the comprehension of the dataset which comprises several compounds and color parameters. Hop color modified greatly in the temperature range with the discoloration more prominent at 70 and 40 °C. The parameter a* is the chromaticity coordinate of the CIELAB color space diagram (Supplementary Material, Fig. S2) that ranges from green (- a) to red (+ a) [33]. a* values increased in all temperatures, representing the green color degradation from fresh green towards green-brown due to the chlorophyll degradation by heat and oxidation [34]. Interestingly, the difference was higher in the lower temperatures (Supplementary File, Table S4) which evidences the great effect of prolonged drying time on green color degradation. Therefore, controlling the termination period of drying could reduce the color degradation in hops and, consequently, enhance the product quality.

Hop total essential oil became one of the main requirements for good quality due to the high demand for hoppy aroma in beer. However, the total essential oil content was greatly affected by the drying process, decreasing by 65.8 % when dried at 70 °C (Supplementary File, Table S3). Figure 3 a-c demonstrates that the total essential oil content decreases considerably with the temperature increase. Despite extended time at 40 °C, this condition represented the lowest difference in the total essential oil content between the fresh and dried hops. This study's finding demonstrates that the processing time has a lower influence on essential oil maintenance in comparison with the temperature. The essential oil components are heat-labile substances, and the higher temperature increases the heat transfer from the surrounding air to the compounds, achieving faster activation energy to volatile [35]. *Rybka* et al. [36, 37] demonstrated the greater effect of drying temperature on the hop essential oil preservation as well as hop quality. In their study, a Saaz variety dried at 40 °C lost 13.6 % of total essential oil content in comparison with 47.0 % when hop was dried at 60 °C. However, *Rubottom* et al. [38] showed that drying temperature impact is variety- and crop-dependent with lower effect on hop oil composition and sensory evaluation.

As demonstrated in the bar chart in figure 3 a-c, the drying process had no effect on the hop bitter acids and xanthohumol content. The difference in those compounds' content between the fresh hops and the dried ones was proximal to zero in all temperatures, highlighting the thermostability of those compounds. This finding is in concordance with *Sturm* et al. [39] results which confirmed the thermostability of α- and β-acids during the drying regardless of the bulk weight.

Figure 3 d presents the correlation between those chemical analytes measured. Interestingly, total essential oil content represented a high correlation with the color parameters which can be certainly explained by the degradation of color alongside the essential oil content decrease during drying. Hop color is a relevant quality attribute for product acceptance by the consumer and it is also an indicator of the overall product quality. In that sense, Sturm et al. [40] developed an in-process predictive model for moisture content and color with the aid of non-invasive optical sensors. This highlights the feasibility of hop quality enhancement through the usage of modern tools as well as process optimization.

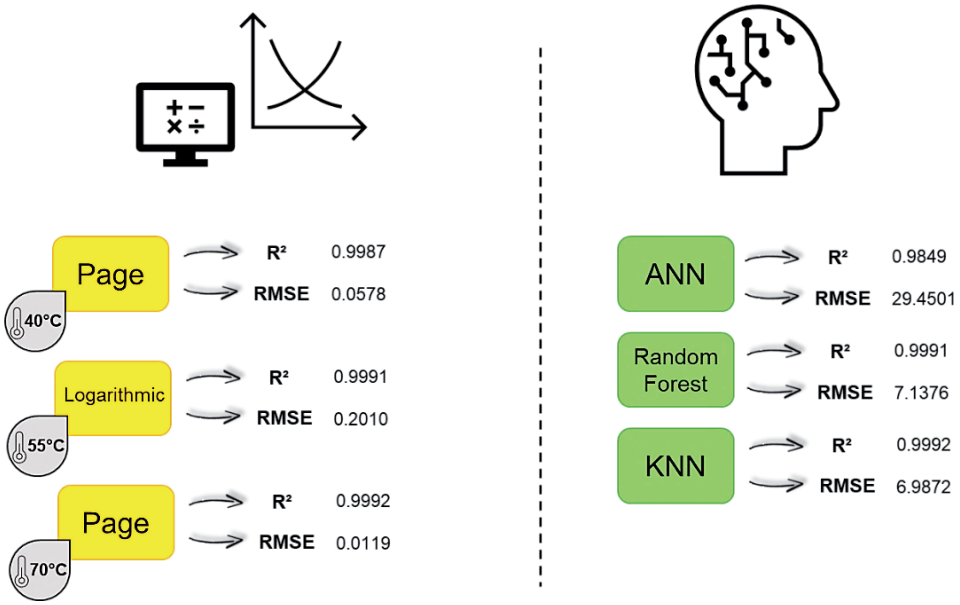

Fig. 4 **R^2 and RMSE values for the best mathematical model fit in each drying temperaturea (left) and the machine learning models (right); [a]The R^2 and RMSE values for all mathematical models are found in Table S1 (Supplementary Material)**

4.2 Comparison of Conventional Mathematical Models and Machine Learning Models

In figure 4, it can be seen that the Page model sufficiently described the moisture ratio prediction for the temperatures of 40 and 70 °C, with higher R^2 values (> 0.999) and lower RMSE values (< 0.06). While for the temperature of 55 °C the logarithmic model fitted greatly the experimental data, due to the higher values of R^2 (>0.999) and lower RMSE values (<0.03). The findings of the current study are consistent with those of *Demir* et al. [41] study which found suitability in Page's model for predicting the moisture rate in bay leaves drying kinetics. Furthermore, *Darvish* et al. [42] dill leaf drying study demonstrated that the logarithmic model offered the best fit to the experimental data in drying kinetics.

The prediction of drying time presented higher accuracy of the KNN and Random Forest model with a higher R^2 value (>0.999) and lower RMSE (< 7.5) in comparison with the ANN model (R^2 < 0.999) (Fig. 4). As expected, the Random Forest algorithm fitted the experimental data sufficiently due to its capacity to build a randomized decision tree in each iteration of the bagging algorithm, producing excellent predictors [14]. The KNN algorithm is described in the literature as a lazy classifier and is usually slower than Random Forest and Multilayer Perceptron algorithms. However, in this study, the KNN algorithm completed the model in less than 1 second, whereas the Random Forest and ANN algorithms took 1.82 and 3.59 seconds, respectively. Therefore, for this dataset, the KNN algorithm demonstrated reasonable performance regarding computational execution and reduced error rates. The best fit occurred with the Random Forest and KNN models due to the reduced error rate and fewer data dissipation (Fig. 5). Pearson's correlation of these models is 0.9991 and 0.9992 with R^2 values of 0.9982 and 0.9983, respectively. On the other hand, Pearson's correlation for the ANN model stands out at 0.9829 with an R^2 value of 0.9658, demonstrating the model's reduced ability for data fitting and prediction.

Although Page's model at 70 °C and the logarithmic model at 55 °C achieved similar correlation coefficient values to the KNN model, their time prediction demonstrates limited regarding the process parameters used. The empirical mathematical modeling predicts the moisture ratio instead of drying time. The drying time calculation adds complexity to the time prediction through both the Page's and logarithmic models [23]. In this case, would be necessary to integrate several assumptions which could reduce the prediction accuracy as well as adding needless effort. Therefore, the machine learning model is suitable for non-linear datasets and facilitates the construction of a complex model using more attributes. Furthermore, this study used open-source software, to facilitate the user's comprehension, which could be implemented in the computers on the farm. Once the model is constructed, an output (drying time) is generated by the addition of new inputs. However, further investigation must be performed to validate this model to other datasets, since the results obtained in this study are specifically for the dataset used.

4.3 Implications of using machine learning to predict the drying time of hops

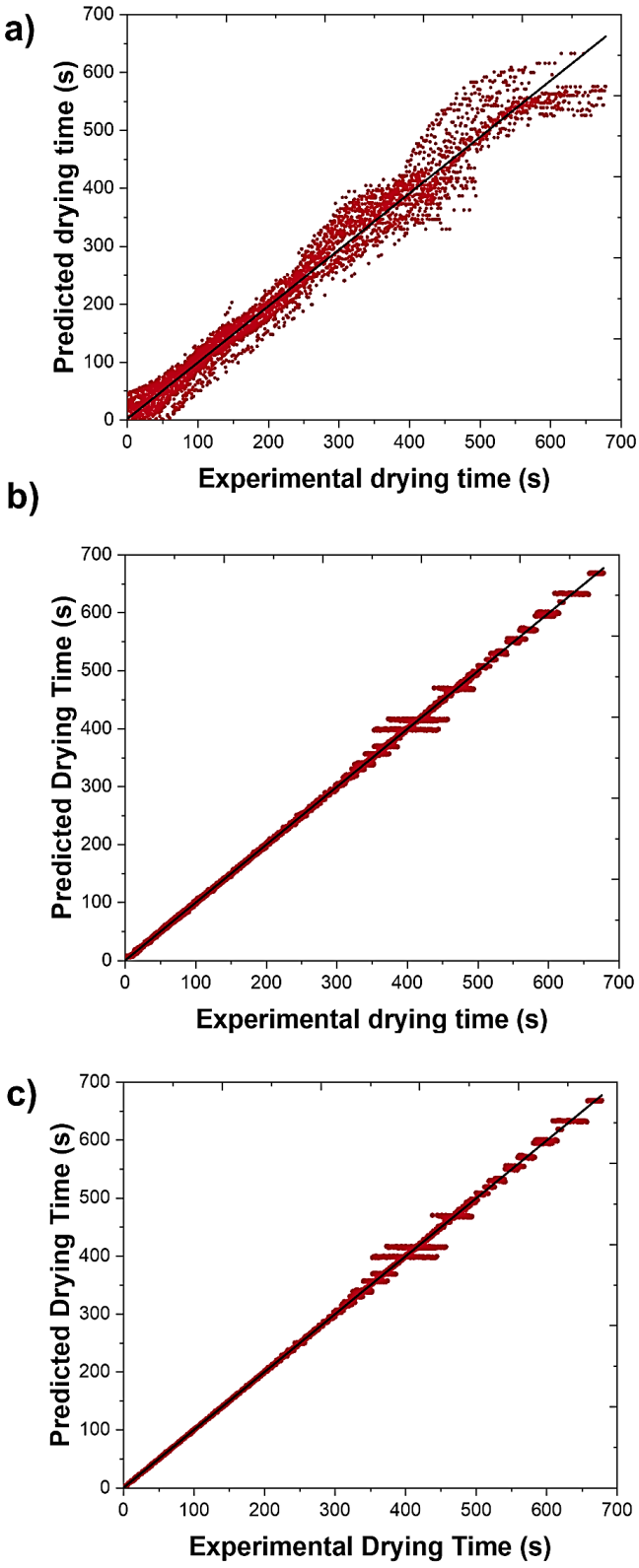

Fig. 5 Predicted versus experimental drying time using the 10 cross-validation folds: a) ANN model; b) Random Forest model; c) KNN model

As shown in figure 6, the effective moisture diffusivity coefficient (D_{eff}) has a clear correlation with the air temperature, increasing 3-folds when the temperature shifts from 40 to 70 °C. Generally, the values for agricultural or food products are placed between 10^{-12} and 10^{-8} [43]. A study by *Khaled* et al. [44] found similar results for the persimmon fruit D_{eff}, ranging from 1.3×10^{-9} to 9.2×10^{-9}. There-

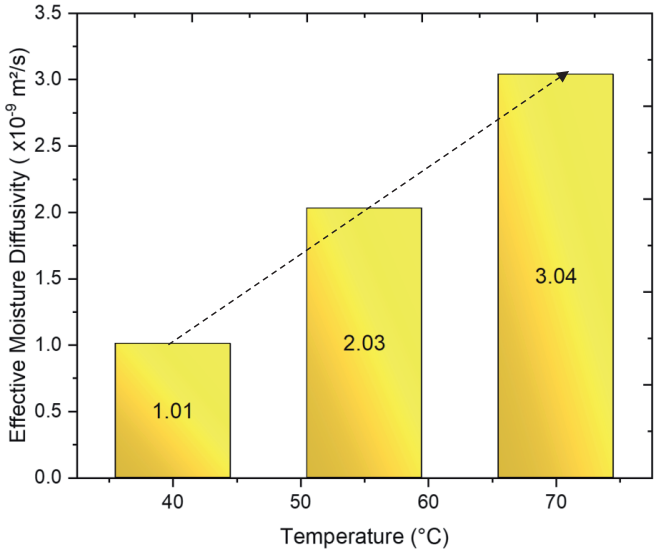

Fig. 6 Effect of air temperature on the effective moisture diffusion coefficient

fore, the values found for the hop cones are within the expected. Diffusivity is defined as the moisture transport phenomenon in food and is described by Fick's law [23, 45]. Elevated air temperatures lead to higher heat transfer to inner water which flows rapidly to the surface [23]. The D_{eff} increases at a higher temperature due to the water molecule's diffusional movement over a shorter time. However, high temperatures and increased D_{eff} lead to profound texture changes during the process. In hops, the bracts contain lower moisture content whereas string has higher moisture and is placed inner the cones, coming into less contact with the surrounding air [46]. During drying, bracts dry more rapidly than the string and, consequently, culminate in different final moisture [47]. By extending the exposure time, hop cones undergo over-drying that causes shatter due to the glass transition, especially in the bracts, to a vitreous state [48]. In that case, hop cones tend to lose more lupulin gland along with the main hop compounds, devaluating the product.

The activation energy was obtained by the Arrhenius-type equation. The value for hops was found to be 30.784 kJ/mol, within the expected range of activation energy. For agricultural and food products, an amount of activation energy between 12.7 and 110 kJ/mol is expected [43]. Activation energy is the minimum amount necessary to initiate water flow from the product to the surface and it is directly correlated to diffusivity [49].

Machine learning has been widely used for prediction in the past decades, allowing elevated accuracy along with reduced efforts. During the drying process, time and temperature are the main parameters that influence efficiency and energy expenditure. Nevertheless, climate conditions demonstrate a large effect on the drying performance due to water diffusivity to the outer air as well as the moisture transfer rate from inside the product to the surrounding air, represented by D_{eff}. Therefore, the machine learning models were built using not only the common parameters as attributes (temperature, and moisture rate) but also the environmental measurements (dry- and wet-bulb temperature) in order to provide more accurate results for process improvement at the hop farm. The machine learning model presented in that study could be improved by the addition of further weather conditions and process parameters, such as environmental moisture, inner product temperature, and air velocity. Furthermore, a scale-up study is recommended to validate the machine learning model for real setup conditions.

The machine learning modeling as developed in that study permits drying time reduction due to sharp control using additional process variables, enhancing the product quality. Diminished drying time enables producers to increase daily production, resulting in lower cone mold deterioration after harvesting due to reduced storage time at a higher moisture content [6]. Drying process optimization by machine learning produces high-quality hops with minimal energy expenditure, reducing over-drying. The drying step leads to a higher carbon footprint in the hops processing [50]; therefore, avoiding energy expenses is paramount to reducing greenhouse gas emissions as well as minimizing costs.

5 Conclusion

For the first time, this study proposed using machine learning as a modeling tool for predicting the drying time of hops, which might be a key to improving the process in a more sustainable and economical direction. The performance of machine learning and empirical models was similar; however, the KNN model was able to describe a wider range of experimental data, whereas the application of empirical models is limited to fewer attributes. Machine learning has the advantage of considering not only the common parameters (temperature, and moisture rate) but also environmental measurements (dry- and wet-bulb temperature) which greatly affects hop drying performance. However, there is still room to improve the methodology proposed here, by extensive research using further weather conditions and process parameters that were not considered in this study, as well as exploring the process scale-up with other hop varieties and validation with other datasets.

Acknowledgment

The authors wish to acknowledge the Van den Bergen company for the material donated.

Conflict of interest

The authors have no conflict of interest.

Funding sources

The authors appreciate the support of the CNPq – Research Nacional Council - Brazil (Finance code 141485/2018-3).

6 References

1. Statista: Worldwide beer production, https://www.statista.com/statistics/270275/worldwide-beer-production/#:~:text=In%202020%2C%20the%20global%20beer,and%20yeast%20as%20basic%20ingredients.
2. Lewis, M.J. and Bamforth, C.W.: Essays in Brewing Science, Springer

Science+Business, New York, 2006.
3. Almaguer, C.; Schönberger, C.; Gastl, M.; Arendt, E.K. and Becker, T.: *Humulus lupulus* – a story that begs to be told. A review, Journal of the Institute of Brewing, **120** (2014), no. 4, pp. 289-314.
4. Barth-Haas Group: Barth Haas Report 2021/222021.
5. Hauser, D.G. and Shellhammer, T.H.: An Overview of Sustainability Challenges in Beer Production, and the Carbon Footprint of Hops Production, Technical Quarterly, 2019.
6. Biendl, M.; Engelhard, B.; Forster, A.; Gahr, A.; Lutz, A.; Mitter, W.; Schmidt, R. and Schönberger, C.: Hops: their Cultivation, Composition, and Usage, Fachverlag Hans Carl GmbH, Nuremberg, 2014.
7. Rourke, B.T.O.: Hops and hop products, The brewer international, **3** (2003), no. 1, pp. 21-25.
8. Sun, Q.; Zhang, M. and Mujumdar, A.S.: Recent developments of artificial intelligence in drying of fresh food: A review, Critical Reviews in Food Science and Nutrition, **59** (2019), no. 14, pp. 2258-2275.
9. Lewis, W.K.: The Rate of Drying of Solid Materials, Industrial and Engineering Chemistry, **13** (1921), no. 5, pp. 427-432.
10. Page, G.E.: Factors Influencing the Maximum Rates of Air Drying Shelled Corn in Thin Layers1949.
11. Yagcioglu, A.K.; Degirmencioglu, A. and Cagatay, F.: Drying Characteristics of Laurel Leaves Under Different Drying Conditions, 7th Int Congress Agricultural Mechanisation and Energy, Adana, 1999, pp. 565-569.
12. Henderson, S.M.: Progress in Developing the Thin Layer Drying Equation., Transactions of the American Society of Agricultural Engineers, **17** (1974), no. 6, pp. 1-3.
13. Karathanos, V.T.: Determination of water content of dried fruits by drying kinetics, Journal of Food Engineering, **39** (1999), no. 4, pp. 337-344.
14. Witten, I.H. and Frank, E.: Data Mining: Practical Machine Learning Tools and Techniques, 2nd ed., Elsevier Inc., London, 2011.
15. Jahanbakhshi, A.; Momeny, M.; Mahmoudi, M. and Radeva, P.: Waste management using an automatic sorting system for carrot fruit based on image processing technique and improved deep neural networks, Energy Reports, **7** (2021), pp. 5248-5256.
16. Abbaspour-Gilandeh, Y.; Jahanbakhshi, A. and Kaveh, M.: Prediction kinetic, energy and exergy of quince under hot air dryer using ANNs and ANFIS, Food Science and Nutrition, **8** (2020), no. 1, pp. 594-611.
17. Jahanbakhshi, A.; Abbaspour-Gilandeh, Y.; Heidarbeigi, K. and Momeny, M.: Detection of fraud in ginger powder using an automatic sorting system based on image processing technique and deep learning, Computers in Biology and Medicine, **136** (2021).
18. Golpour, I.; Kaveh, M.; Amiri Chayjan, R. and Guiné, R.P.F.: Optimization of Infrared-convective Drying of White Mulberry Fruit Using Response Surface Methodology and Development of a Predictive Model through Artificial Neural Network, International Journal of Fruit Science, (2020), pp. 1-21.
19. Khaled, A.Y.; Kabutey, A.; Mizera, C.; Hrabe, P. and Herák, D.: Modelling of hot-air and vacuum drying of persimmon fruit (Diospyros kaki) using computational intelligence methods, Agronomy Research, **18** (2020), no. Special Issue 2, pp. 1323-1335.
20. Technical Committe, A.: Hops - 4: Moisture, ASBC Methods of Analysis, 2011, pp. 1-2.
21. Karakaplan, N.; Goz, E.; Tosun, E. and Yuceer, M.: Kinetic and artificial neural network modeling techniques to predict the drying kinetics of Mentha spicata L., Journal of Food Processing and Preservation, **43** (2019), no. 10, pp. 1-10.
22. Berk, Z.: Food Process Engineering and Technology, 3rd ed., Elsevier, 2018.
23. Kerr, W.L.: Handbook of Farm, Dairy and Food Machinery Engineering, 2nd ed., Elsevier Inc., London, 2013.
24. Chen, Y.-C.; Chung, J.-H.; Yeh, Y.-J.; Lou, S.-J.; Lin, H.-F.; Lin, C.-H.; Hsien, H.-H.; Hung, K.-W.; Yeh, S.-C.J. and Shi, H.-Y.: Predicting 30-Day Readmission for Stroke Using Machine Learning Algorithms: A Prospective Cohort Study, Frontiers in Neurology, **13** (2022).
25. Kristinsson, Æ.Ö.; Gu, Y.; Rasmussen, S.M.; Mølgaard, J.; Haahr-Raunkjær, C.; Meyhoff, C.S.; Aasvang, E.K. and Sørensen, H.B.D.: Prediction of serious outcomes based on continuous vital sign monitoring of high-risk patients, Computers in Biology and Medicine, **147** (2022), p. 105559.
26. Chen, S.-D.; You, J.; Yang, X.-M.; Gu, H.-Q.; Huang, X.-Y.; Liu, H.; Feng, J.-F.; Jiang, Y. and Wang, Y.: Machine learning is an effective method to predict the 90-day prognosis of patients with transient ischemic attack and minor stroke, BMC Medical Research Methodology, **22** (2022), no. 1, p. 195.
27. Chen, S.-D.; You, J.; Yang, X.-M.; Gu, H.-Q.; Huang, X.-Y.; Liu, H.; Feng, J.-F.; Jiang, Y. and Wang, Y.: Machine learning is an effective method to predict the 90-day prognosis of patients with transient ischemic attack and minor stroke, BMC Medical Research Methodology, **22** (2022), no. 1, p. 195.
28. Son, J.; Kim, D.; Na, J.Y.; Jung, D.; Ahn, J.-H.; Kim, T.H. and Park, H.-K.: Development of artificial neural networks for early prediction of intestinal perforation in preterm infants, Scientific Reports, **12** (2022), no. 1, p. 12112.
29. Nasser, I.M. and Abu-Naser, S.S.: Lung Cancer Detection Using Artificial Neural NetworkInternational Journal of Engineering and Information Systems (IJEAIS), 2019.
30. Breiman, L.: Random forests, Machine Learning, **45** (2001), pp. 5-32.
31. Aha, D.W.; Kibler, D. and Albert, M.K.: Instance-Based Learning Algorithms, Machine Learning, **6** (1991), pp. 37-66.
32. Kohavi, R.: Wrappers for Performance Enhancement and Oblivious Decision Graphs, 1995.
33. Ly, B.C.K.; Dyer, E.B.; Feig, J.L.; Chien, A.L. and Del Bino, S.: Research Techniques Made Simple: Cutaneous Colorimetry: A Reliable Technique for Objective Skin Color MeasurementJournal of Investigative Dermatology, 2020.
34. Bonazzi, C. and Dumoulin, E.: Quality Changes in Food Materials as Influenced by Drying Processes, Modern Drying Technology, 2011.
35. Damodaran, Srinivasan.; Parkin, K.L. and Fennema, O.R.: Química de alimentos de Fennema (4a. ed.)., Grupo A - Artmed, 2000.
36. Rybka, A.; Krofta, K.; Heřmánek, P.; Honzík, I. and Pokorný, J.: Effect of drying temperature on the content and composition of hop oils, Plant, Soil and Environment, **64** (2018), no. 10, pp. 512-516.
37. Rybka, A.; Heřmánek, P. and Honzík, I.: Effect of drying temperature in hop dryer on hop quality, **67** (2021), no. 1, pp. 1-7.
38. Rubottom, L.N.; Lafontaine, S.R.; Hauser, D.G.; Pereira, C.; Shellhammer, T.H.: Hop Kilning Temperature Sensitivity of Dextrin- Reducing Enzymes in Hops, Journal of the American Society of Brewing Chemists, **80** (2021), no. 1, pp. 1-13.
39. Raut, S.; Gersdorff, G.J.E. von; Münsterer, J.; Kammhuber, K.; Hensel, O. and Sturm, B.: Impact of Process Parameters and Bulk Properties on Quality of Dried Hops, Processes, **8** (2020), no. 11, p. 1507.
40. Sturm, B.; Raut, S.; Kulig, B.; Münsterer, J.; Kammhuber, K.; Hensel, O. and Crichton, S.O.J.: In-process investigation of the dynamics in drying behavior and quality development of hops using visual and environmental sensors combined with chemometrics, Computers and Electronics in Agriculture, **175** (2020), p. 105547.
41. Demir, V.; Gunhan, T.; Yagcioglu, A.K. and Degirmencioglu, A.: Math-

ematical Modelling and the Determination of Some Quality Parameters of Air-dried Bay Leaves, Biosystems Engineering, **88** (2004), no. 3, pp. 325-335.
42. Darvishi, H.; Farhudi, Z. and Behroozi-Khazaei, N.: Mass Transfer Parameters and Modeling of Hot Air Drying Kinetics of Dill Leaves, Chemical Product and Process Modeling, **12** (2016), no. 2, pp. 1-15.
43. Kaveh, M. and Amiri Chayjan, R.: Modeling Thin-Layer Drying of Turnip Slices Under Semi-Industrial Continuous Band Dryer, Journal of Food Processing and Preservation, **41** (2015), no. 2, pp. 1-14.
44. Khaled, A.Y.; Kabutey, A.; Selvi, K.Ç.; Mizera, Č.; Hrabe, P. and Herák, D.: Application of computational intelligence in describing the drying kinetics of persimmon fruit (*Diospyros kaki*) during vacuum and hot air drying process, Processes, **8** (2020), no. 5.
45. Khan, M.I.H.; Sablani, S.S.; Joardder, M.U.H. and Karim, M.A.: Application of machine learning-based approach in food drying: opportunities and challenges, Drying Technology, **40** (2020), no. 6, pp. 1-17.
46. Münsterer, J.: Optimale Trocknung und Konditionierung von Hopfen, LfL Information2006.
47. Raut, S.; Gersdorff, J.E. Von; Münsterer, J.; Kammhuber, K.; Hensel, O. and Sturm, B.: Influence of pre-drying storage time on essential oil components in dried hops (*Humulus lupulus* L.), Journal of the Science of Food and Agriculture, **101** (2020), no. 6, pp. 2247-2255.
48. Fellows, P.: Food processing technology : principles and practice, Second Edition ed., Woodhead Publishing Limited, Cambridge, England, 2002.
49. Koukouch, A.; Idlimam, A.; Asbik, M.; Sarh, B.; Izrar, B.; Bostyn, S.; Bah, A.; Ansari, O.; Zegaoui, O. and Amine, A.: Experimental determination of the effective moisture diffusivity and activation energy during convective solar drying of olive pomace waste, Renewable Energy, **101** (2017), pp. 565-574.
50. Martynenko, A. and Misra, N.N.: Machine learning in drying, Drying Technology, **38** (2020), no. 5-6, pp. 596-609.

Received 11 January 2023, accepted 24 May 2023

Supplementary Material

Table S1 Correlation coefficient and Root Mean Squared Error values to the fitted model

Absolute Temperature	Model	R^2	RMSE
40 °C	Newton	0.9867	0.6078
	Page	0.9987	0.0578
	Logarithmic	0.9979	0.0927
	Two terms	0.9919	0.3685
	Henderson e Pabis modified	0.9919	0.3685
55 °C	Newton	0.9837	0.3701
	Page	0.9989	0.0230
	Logarithmic	0.9991	0.0210
	Two terms	0.9914	0.1949
	Henderson e Pabis modified	0.9914	0.1949
70 °C	Newton	0.9877	0.1910
	Page	0.9992	0.0119
	Logarithmic	0.9975	0.0383
	Two terms	0.9942	0.0901
	Henderson e Pabis modified	0.9942	0.0901

Fig. S1 The system used for the drying trials

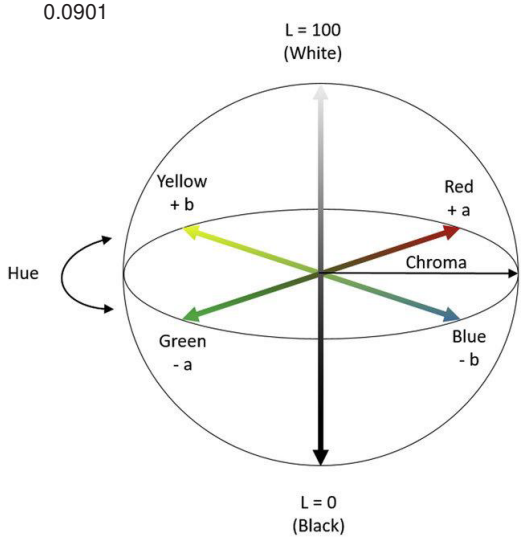

Fig. S2 CIE L* a* b* color space diagram (Ly et al., 2020)[1]

Table S2 Correlogram's dataset calculated with Pearson's correlation

Person's correlation calculated with hop quality dataset											
a*	– 0.17	– 0.99	– 0.92	– 0.35	– 0.26	– 0.05	0.04	0.55	0.77	0.90	1.00
b*	– 0.58	– 0.93	– 0.83	0.02	0.13	0.37	0.46	0.86	0.95	1.00	-
Xanthohumol	– 0.69	– 0.81	– 0.80	0.05	0.18	0.45	0.55	0.93	1.00	-	-
Colupulone	– 0.90	– 0.61	– 0.53	0.41	0.52	0.74	0.81	1.00	-	-	-
N+Adhumulone	– 0.98	– 0.12	0.05	0.85	0.91	0.99	1.00	-	-	-	-
Total Alpha-Acids	– 0.95	– 0.03	0.17	0.91	0.96	1.00	-	-	-	-	-
N+Adlupulone	– 0.82	0.18	0.42	0.99	1.00	-	-	-	-	-	-
Cohumulone	– 0.74	0.27	0.53	1.00	-	-	-	-	-	-	-
Total Essential Oil	0.12	0.90	1.00	-	-	-	-	-	-	-	
L*	0.26	1.00	-	-	-	-	-	-	-	-	-
Total Betal-Acids	1.00	-	-	-	-	-	-	-	-	-	-
	Total Beta-Acids	L*	Total Essential Oil	Cohumulone	N+Adlupulone	Total Alpha-Acids	N+Adhumulone	Colupulone	Xanthohumol	b*	a*

The parameters L, a*, and b* corresponding to color CIELAB parameters: L* value indicates lightness, a* and b* are chromaticity coordinates

Table S3 Average of hop composition and color parameters of fresh and dried hops

Treatment	Color			Bitter Acids						Xanthohumol (%)	Essential Oil
	L*	a*	b*	Total Alpha-Acids	Cohumulone	N+Adhumulone	Total Beta-Acids	Colupulone	N+Adlupulone		Total Essential Oil (mL/100 g)
Fresh Hops	63,41	-1,05	34,47	3,36	0,79	2,57	2,67	1,37	1,30	0,26	1,52
40°C	57,26	3,39	35,34	3,12	0,72	2,40	2,83	1,34	1,18	0,27	0,79
55°C	57,49	3,02	35,88	3,26	0,73	2,52	2,66	1,45	1,22	0,3	0,66
70°C	54,77	4,53	36,72	3,46	0,79	2,67	2,52	1,51	1,32	0,31	0,52

Table S4 Hop quality evaluation by the difference between fresh and dried hops

Treatment		Fresh Hops	40°C	55°C	70°C	Difference (40°C – Fresh Hops)	Difference (40°C – Fresh Hops) %	Difference (55°C – Fresh Hops)	Difference (55°C – Fresh Hops) %	Difference (70°C – Fresh Hops)	Difference (70°C – Fresh Hops) %
Color	L*	63,41	57,26	57,49	54,77	– 6,15	– 0,11	– 5,92	– 0,10	– 8,64	– 0,16
	a*	– 1,05	3,39	3,02	4,53	4,44	1,31	4,07	1,35	5,58	1,23
	b*	34,47	35,34	35,88	36,72	0,87	0,02	1,41	0,04	2,25	0,06
Bitter Acids	Total Alpha-Acids	3,36	3,12	3,26	3,46	– 0,23	– 0,07	– 0,10	– 0,03	0,10	0,03
	Cohumulone	0,79	0,72	0,73	0,79	– 0,07	– 0,10	– 0,06	– 0,08	0,00	0,00
	N+Adhumulone	2,57	2,40	2,52	2,67	– 0,17	– 0,07	– 0,05	– 0,02	0,10	0,04
	Total Beta-Acids	2,67	2,83	2,66	2,52	0,16	0,06	– 0,01	0,00	– 0,15	– 0,06
	Colupulone	1,37	1,34	1,45	1,51	– 0,03	– 0,02	0,08	0,05	0,15	0,10
	N+Adlupulone	1,30	1,18	1,22	1,32	– 0,12	– 0,10	– 0,09	– 0,07	0,01	0,01
	Xanthohumol (%)	0,26	0,27	0,30	0,31	0,01	0,04	0,04	0,13	0,05	0,16
Essential Oil	Total Essential Oil (mL/100g)	1,52	0,79	0,66	0,52	– 0,73	– 0,92	– 0,86	– 1,30	– 1,00	– 1,92

*Difference calculated from the values at 70 °C-FH, 55 °C-FH, and 40 °C-FH